(18). In this study, we analyzed in vivo infection of a popular picornavirus, PV, using PVR transgenic (PVRtg) mice, which show a neurotropic phenotype during PV infection similar to humans (19, 20). Using this mouse model, in combination with TICAM-1$^{-/-}$ or IPS-1$^{-/-}$ mice, we present evidence that the host TICAM-1 pathway, particularly in macrophages (Mf), serves as a source of type I IFN induction and protects host PVRtg mice from PV infection and paralytic death. Thus, the strategy for host protection against picornaviruses is not simply based on the MDA5-dependent dsRNA recognition, but is variable depending on picornavirus species.

Materials and Methods

Mice

All mice were backcrossed with C57BL/6 mice more than seven times before use. TICAM-1$^{-/-}$ (21) and IPS-1$^{-/-}$ mice (this study) were generated in our laboratory. TLR3$^{-/-}$ (4), IRF-3$^{-/-}$, and IRF-7$^{-/-}$ mice (22) were provided by Drs. S. Akira (Osaka University, Osaka, Japan) and T. Taniguchi (University of Tokyo, Tokyo, Japan). PVRtg mice were provided as reported previously (20). All mice were maintained under specific pathogen-free conditions in the Animal Facility at Hokkaido University Graduate School of Medicine (Sapporo, Japan). Animal experiments were performed according to the guidelines set by the Animal Safety Center, Japan.

Generation of IPS-1–deficient mice

The *IPS-1* gene was amplified by PCR using genomic DNA extracted from embryonic stem cells. The targeting vector was constructed by replacing the second and third exons with a neomycin-resistance gene cassette (Neo), and an HSV thymidine kinase driven by the PGK promoter was inserted into the genomic fragment for negative selection. After the targeting vector was transfected into 129/Sv mice-derived embryonic stem cells, G418 and ganciclovir doubly resistant colonies were selected and screened by PCR. The targeted cell line was injected into C57BL/6 blastocysts, resulting in the birth of male chimeric mice. These mice were then backcrossed with C57BL/6 mice. The disruption of the *IPS-1* gene was confirmed by PCR for the long and short arms. The abolishment of IPS-1 mRNA expression was confirmed by real-time quantitative PCR (RT-qPCR).

Cells, viruses, and reagents

Wild-type (WT) and TICAM-1$^{-/-}$ mouse embryonic fibroblasts (MEF) were prepared from 12.5- to 13.5-d-old embryos. PV, strain Mahoney, was amplified in Vero cells, and the viral titer was determined by a plaque assay. Bone marrow (BM) cells were prepared from the femur and tibia. The cells were cultured in RPMI 1640 (Invitrogen, New York, NY) supplemented with 10% FCS, 100 μM 2-ME, and 10 ng/ml murine GM-CSF or the culture supernatant of NIH3T3 cells expressing M-CSF. After 6 d, cells were collected and used as bone marrow-derived dendritic cells (BM-DC) or BM-derived macrophages (BM-Mf). For the preparation of BM-DC and BM-Mf, the medium was changed every 2 d. Splenic DC and NK cells were isolated using the MACS system (Miltenyi Biotec, Auburn, CA).

Experimental infection of mice

Five- to 8-wk-old C57BL/6 female mice were used throughout this study. Mice of different genotypes were i.p. or i.v. infected with PV at the doses indicated. The viability of the infected mice was monitored for 2 wk. We collected sera from the mice at different time points to measure viral titers by a plaque assay and cytokine levels by an ELISA. To determine the tissue viral titer, mice were euthanized and organs were aseptically removed and frozen by liquid nitrogen. Because the organs were not perfused before organs were removed, virus titers were determined including blood. Specimens were homogenized in 2 ml PBS on ice, and titers were determined by a plaque assay.

ELISA

Culture supernatants of cells (10^5) seeded on 24-well plates or sera were collected and analyzed for cytokine levels with ELISA. ELISA kits for IFN-α and IFN-β were purchased from PBL Biomedical Laboratories. ELISA was performed according to the manufacturer's instructions.

qPCR

For qPCR, total RNA was extracted with TRIzol (Invitrogen), and 0.2–0.5 μg RNA was reverse-transcribed using a high-capacity cDNA transcription kit (Applied Biosystems, Piscataway, NJ) with random primers according to the manufacturer's instructions. qPCR was performed using a Step One real-time PCR system (Applied Biosystems).

In vivo blocking of NK activity

Mice (PVRtg and PVRtg/TICAM-1$^{-/-}$) were i.p. injected with 250 μg anti-NK1.1 Ab, asialoGM1 Ab, or control PBS as described previously (21). One day later, the mice were i.p. inoculated with 10^4 PFU PV. One to 7 d after PV injection, depletion of peripheral NK1.1$^+$ cells was confirmed by flow cytometry. Then, the mortality of the mice was monitored. In some experiments, the spleen cells were harvested and NK cells (DX5$^+$ cells) were positively isolated using the MACS system (Miltenyi Biotec). The DX5$^+$ NK cells were suspended in RPMI 1640 containing 10% FCS and mixed with ^{51}Cr-labeled B16D8 cells at the indicated E:T ratios. After 4 h, the supernatants were harvested and [^{51}Cr] release was measured.

Statistical analysis

Statistical significance of differences between groups was determined by the Student *t* test, and survival curves were analyzed by the log-rank test using Prism 4 for Macintosh software (GraphPad Software). Student *t* tests and χ^2 goodness-of-fit tests were performed using Microsoft Excel software and a χ^2 distribution table.

Results

TICAM-1 is essential for protection of PVRtg mice against PV infection

Mice lacking the *mda-5* gene abrogate the production of type I IFN in response to EMCV infection and are more susceptible to infection with EMCV (13, 17). Because EMCV is a picornavirus, it has been proposed that MDA5 is critical for sensing picornavirus infection. In infected cells, picornaviruses efficiently generate long dsRNA, which is recognized by the cytoplasmic dsRNA sensor MDA5 (23). The 5′ end of the PV genomic RNA is linked to a VPg protein (16), not to a 5′-triphosphate, a major ligand for another cytoplasmic RNA sensor, RIG-I (24, 25). Thus, we first tested, using the PVRtg mouse model (20), whether the mortality of PV-infected mice is affected by disruption of IPS-1 (Fig. 1*A*). Approximately 70% of WT (PVRtg) mice and ~40% of IPS-1$^{-/-}$ mice survived >10 d postinoculation at an i.p. dose of 2×10^4 PFU. No statistical significance between these two groups was detected (Fig. 1*A*). In the same experiments, TICAM-1$^{-/-}$ mice died within 5 d by paralysis (Fig. 1*B*).

We next investigated the effect of the route of PV infection on mortality in this mouse model. PV (2×10^3 PFU) was injected i.p. or i.v. into WT and TICAM-1 mice and their mortality was examined (Fig. 1*C*, 1*D*). All TICAM-1$^{-/-}$ mice died by paralysis within 7.5 d irrespective of the injection route. The significance of this early mortality rate of PV-infected TICAM-1$^{-/-}$ mice was supported by statistical analysis. The mortality rates were slightly high in WT mice compared with IPS-1$^{-/-}$ mice when PV loads in mice were not very high (Supplemental Fig. 1*A*). This tendency seemingly diminished by early death of IPS-1$^{-/-}$ mice with high doses of PV input. These data suggested that TICAM-1, rather than IPS-1 (or the sensors RIG-I and MDA5), is a critical factor in protecting mice from PV-mediated paralytic death. This conclusion was confirmed using RIG-I$^{-/-}$ and MDA5$^{-/-}$ mice with a PVRtg background (S. Abe, K. Fujii, and S. Koike, submitted for publication).

These results showed a discrepancy with previous indications that MDA5 is critical in picornavirus protection (13). We therefore tested the dose dependence of PV in the survival of WT versus TICAM-1$^{-/-}$ mice. Surprisingly, high doses of PV (2×10^5 and 2×10^6 PFU) induced paralytic death in all WT as well as TICAM-1$^{-/-}$ mice within 6 d (Fig. 2*A*, 2*B*). Thus, high doses of PV (>2×10^5 PFU) appear to overpower the TICAM-1 PV-protective activity in vivo, which confirmed previous findings using other picornaviruses (13). TICAM-1 was most effective in

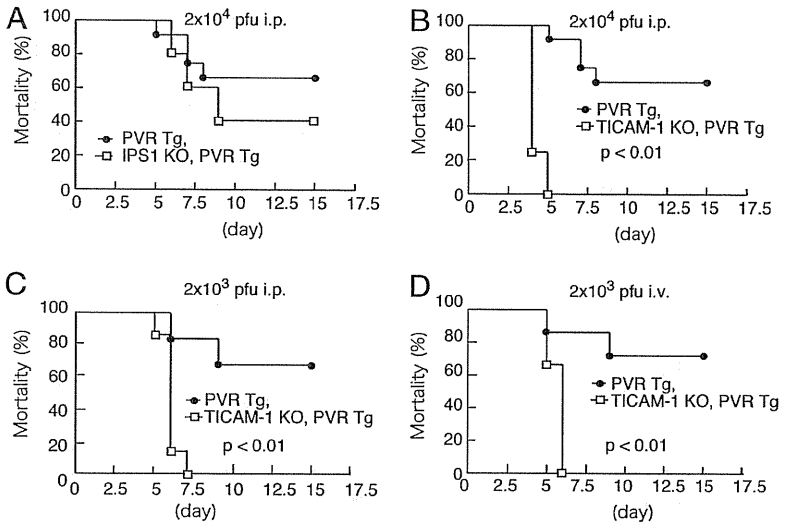

FIGURE 1. Survival of WT, TICAM-1 KO, and IPS-1 KO mice following i.p. or i.v. PV infection. *A* and *B*, PV (2×10^4 PFU) was infected via the i.p. route into WT and IPS-1 (*A*) or TICAM-1 (*B*) KO mice ($n \geq 5$), and survival was monitored for 14 d. *C* and *D*, PV (2×10^3 PFU) was infected via the i.p. (*C*) or i.v. (*D*) route into WT and TICAM-1 KO mice ($n \geq 5$), and survival was monitored for 14 d.

the survival against PV infection at low dose ($<2 \times 10^4$ PFU) (Figs. 1*B*, 1*C*, 2*C*). Similar results were obtained with the PV infection study (S. Abe, K. Fujii, and S. Koike, submitted for publication) when TICAM-$1^{-/-}$ mice were substituted with TLR$3^{-/-}$ or IRF-3/7 double-knockout (KO) mice. Results were confirmed using IRF-$3^{-/-}$ and IRF-$7^{-/-}$ mice (26). These results are essentially consistent with previous reports using a PVRtg/IFNAR$^{-/-}$ mouse model (27), in which type I IFN is critical for PV permissiveness, particularly in the intestine of PVRtg mice.

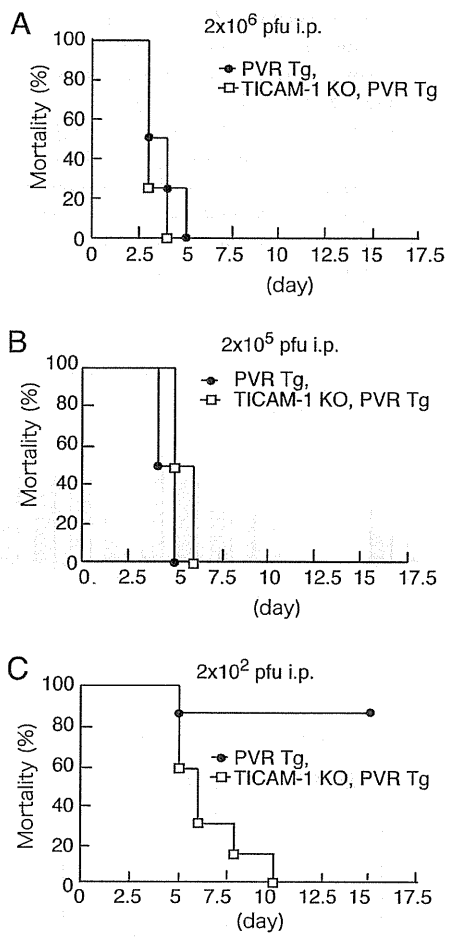

FIGURE 2. High doses of PV disable the protective effect of TICAM-1. WT and TICAM-1 KO mice ($n \geq 6$) were i.p. infected with 2×10^6 (*A*), 2×10^5 (*B*), or 2×10^2 PFU (*C*) PV and survival was monitored for 14 d.

TICAM-1–dependent type I IFN induction in PVRtg mice

PV titers in various organs were measured with WT and TICAM-$1^{-/-}$ mice i.p. injected with 2×10^4 PFU PV. In most organs, PV titers were higher in TICAM-$1^{-/-}$ mice than in WT mice at day 3 post-infection (Fig. 3*A*). The PV titer ratio in TICAM-$1^{-/-}$ versus WT mice was also high in the lung (Fig. 3*A*). In most organs except for the large intestine, high PV titers were harvested in TICAM-$1^{-/-}$ mice compared with WT mice. The difference in local PV titers between WT and TICAM-$1^{-/-}$ mice was culminated in the lung and spinal cord (Fig. 3*A*). Serum PV titers were increased within 48 h

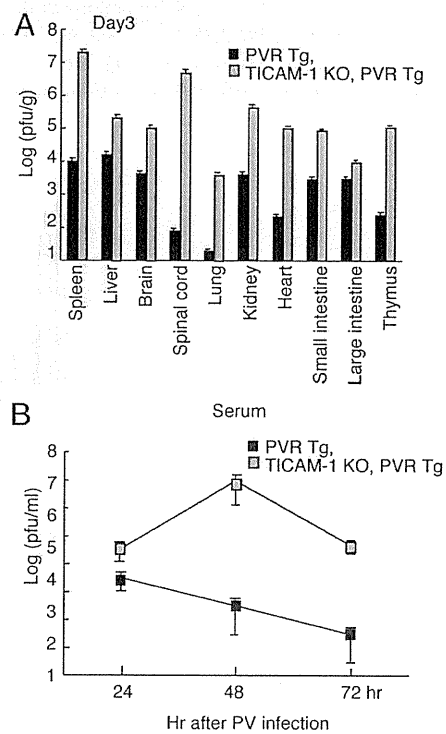

FIGURE 3. Viral titers in organs and serum following PV infection. WT and TICAM-1 KO mice were infected i.p. with 2×10^4 PFU PV. The viral titers in each organ (*A*) and sera (*B*) were measured by a plaque assay. Data are shown as means ± SD of three independent samples.

after PV i.p. injection in TICAM-1$^{-/-}$ mice compared with WT mice (Fig. 3*B*).

IFN-α/β levels were measured with sera from WT, IPS-1$^{-/-}$, and TICAM-1$^{-/-}$ mice, but they were barely detected in these PV-infected mice (Supplemental Fig. 1*B*). Only i.v. injection of high PV titers (an example shows >4 × 10^6 PFU) allowed WT mice to release type I IFN within 12 h (Supplemental Fig. 1*B*). No IFN was detected in blood in TICAM-1$^{-/-}$ and IPS-1$^{-/-}$ mice even in this high-dose setting. However, IFN-α production was reproduced in a cell type level (peritoneal Mf) in vitro (Supplemental Fig. 1*C*). PV infection-mediated cell death (28) and degradation of MDA5 protein (29) may be major causes for this undetectable type I IFN production during in vivo PV infection.

TICAM-1 pathway contributes to IFN-β induction in WT mice with low PV titers

We next determined the mRNA levels of type I IFN in each organ extracted from PV (2 × 10^4 PFU)-infected WT and TICAM-1$^{-/-}$ mice. IFN-β mRNA was upregulated in all of the organs tested in WT mice within 12 h in response to PV injection (i.p.) (Fig. 4*A*). In contrast, only a low increase in IFN-β mRNA was detected in the organs of TICAM-1$^{-/-}$ mice (Fig. 4*A*). IFN-α2 mRNA was upregulated in the organs of TICAM-1$^{-/-}$ and WT mice to similar extents in response to PV injection (2 × 10^4 PFU, i.p.) (Fig. 4*B*). Notable decreases in IFN-α2 mRNA were observed in the TICAM-1$^{-/-}$ spleen and spinal cord compared with WT controls (Fig. 4*B*). The mRNA levels of genes associated with type I IFN induction were evaluated by qPCR, and no unique differences were observed between the splenocytes from PV-injected TICAM-1$^{-/-}$ and IPS-1$^{-/-}$ mice (Supplemental Fig. 1*D*). Hence, type I IFN mRNA is generally upregulated via TICAM-1 in the local organs of PVRtg WT mice during PV infection.

The mRNA levels of IFN-inducible genes and other cytokines were determined in spleen cells after PV infection. IFN-λ and IFN-γ–induced protein 10 (IP-10) mRNA were upregulated in the spleen cells of WT, but not TICAM-1$^{-/-}$ mice, after PV infection (multiplicity of infection [MOI] of 1) (Fig. 4*C*), with profiles similar to that of IFN-β mRNA (Fig. 4*C*). A sensor for 5′-triphosphorylated RNA, IFN-induced protein with tetratripeptide repeats 1 (IFIT-1), was also upregulated through PV infection (Fig. 4*C*). TNF-α, IL-10, IL-12p40, and IFN-γ, which may be associated with infectious cell death, were barely upregulated in spleen cells in response to PV infection (Supplemental Fig. 1*E*).

TICAM-1–dependent type I IFN induction by PV depends on Mf in PVRtg mice

The types of cells that participate in type I IFN induction in the spleen were examined by sorting spleen cells. IFN-β and IFN-α2 were found to be induced in WT CD11c$^+$ DC (Fig. 5*A*), whereas CD11c$^-$ cells barely induced type I IFN. Furthermore, IFN-β and IFN-α2 were barely induced in TICAM-1$^{-/-}$ CD11c$^+$ cells (Fig. 5*B*). Participation of IPS-1 in type I IFN induction in CD11c$^+$ myeloid cells is less compared with that of TICAM-1 (Fig. 5*B*).

Splenic CD8α$^+$CD11c$^+$ and CD4$^+$CD11c$^+$ cells were separated by MACS beads and their response to PV (MOI of 1) was analyzed by determining the mRNA levels of type I IFN (Fig. 5*C*). CD8α$^+$CD11c$^+$ cells, but not the CD4$^+$CD11c$^+$ cells, of WT mice were responsible for type I IFN induction by PV. There was a CD4$^-$CD8α$^-$ population of DC in the spleen and this type of cells did not induce type I IFN in response to PV (Supplemental Fig. 2). The generation of the mRNA of type I IFN and IFIT-1 by PV infection was abrogated in the TICAM-1$^{-/-}$ CD8α$^+$CD11c$^+$ splenic DC (Fig. 5*D*). Also, CD4/8α double-negative DC failed to express type I IFNs (Supplemental Fig. 2). Thus, CD8α$^+$CD11c$^+$ DC, which reportedly express TLR3 (30), are the source of type I IFN in PV-infected PVRtg mice.

We finally confirmed that type I IFN is locally induced in TLR3$^+$ myeloid cells during PV infection. BM-Mf and BM-DC were prepared from mouse BM and challenged with PV (MOI of 1). These cells express TLR3 in the endosome as previously reported about mouse BM-DC (30) and human monocyte-derived DC (31). BM-Mf showed similar profiles of type I IFN mRNA to those of PV-infected splenocytes (Figs. 4*C*, 6*A*). However, IFN-λ and IP-10 mRNA were not detectable in PV-infected BM-Mf, the reason for which remains unclear (Fig. 6*A*). IL-12p40, a representative TICAM-1–dependent gene, was transiently upregulated

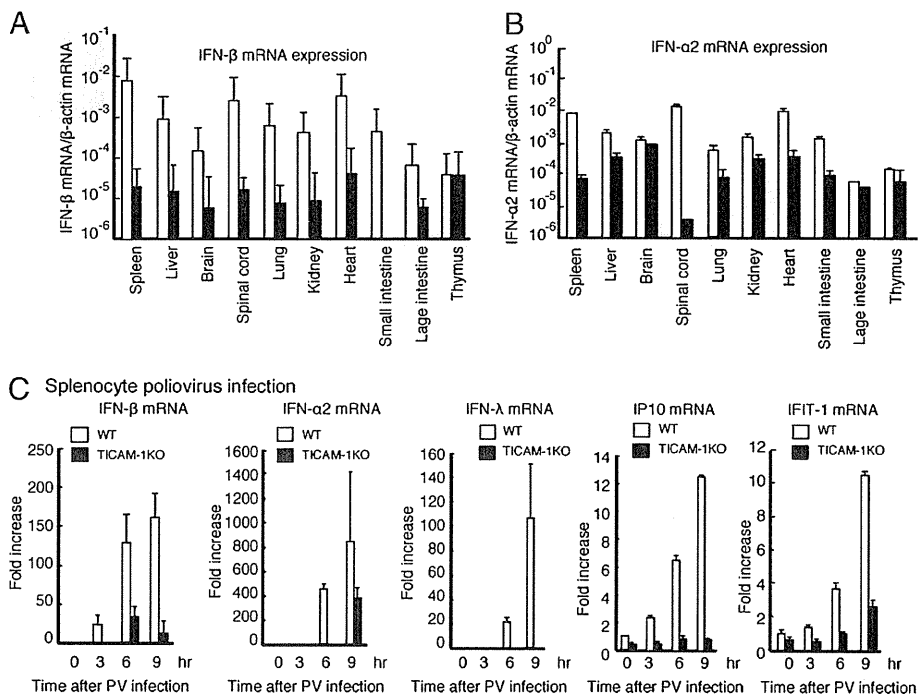

FIGURE 4. The expression of type I IFN following PV infection. *A* and *B*, WT and TICAM-1 KO mice were infected i.p. with 2 × 10^4 PFU PV. Three days postinfection, the mRNA expression levels of IFN-β (*A*) and IFN-α (*B*, *C*) were determined by RT-qPCR. *C*, Splenocytes (5 × 10^5) were infected with PV (MOI of 1) and the mRNA expression levels of IFN-β, IFN-α2, IFN-λ, IP-10, and IFIT-1 were measured by RT-qPCR. Data are shown as means ± SD and are representative of three independent experiments.

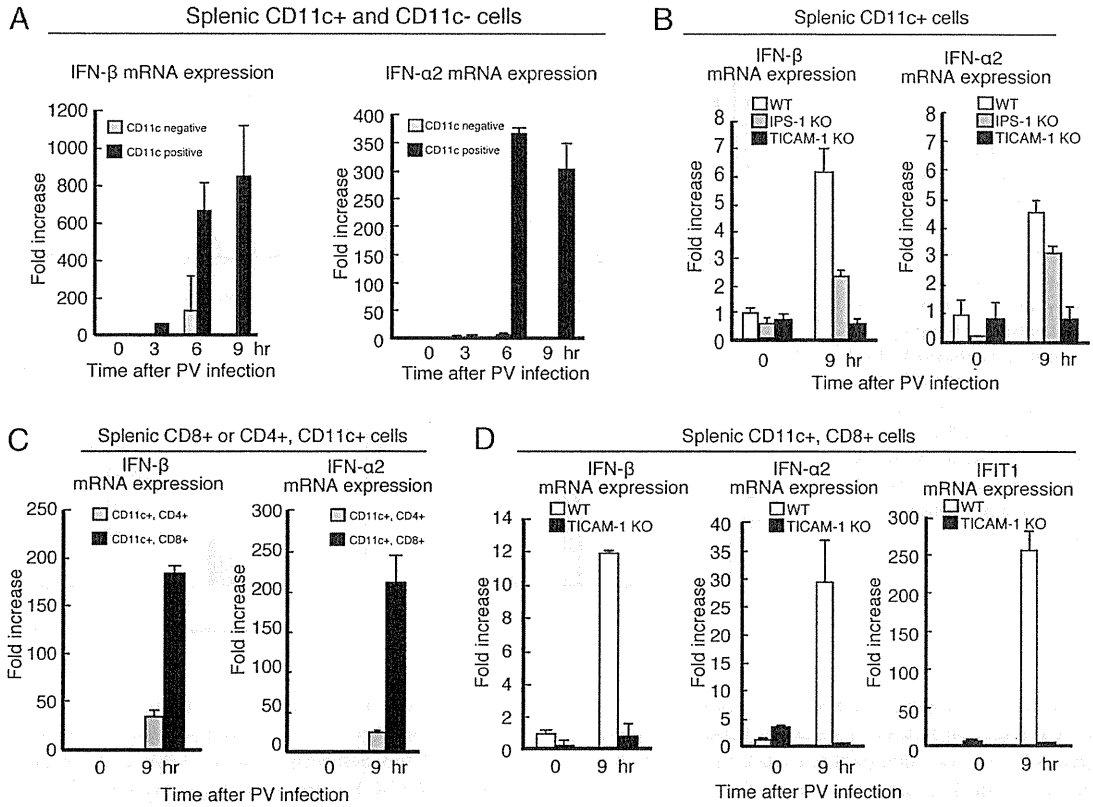

FIGURE 5. The expression of type I IFN in splenic DC. *A*, were isolated from WT spleens using the MACS system. $CD11c^+$ or $CD11c^-$ cells (5×10^5) were infected with PV (MOI of 1), and the mRNA expression of type I IFNs was measured by RT-qPCR. *B*, WT, TICAM-1, and IPS-1 knockout splenic $CD11c^+$ cells were infected with PV, and the expression of type I IFNs was measured by RT-qPCR. *C*, $CD8\alpha^+CD11c^+$ cells and $CD4^+CD11c^+$ cells were isolated from WT spleens and infected with PV (MOI of 1). The expression of type I IFNs was measured by RT-qPCR. *D*, $CD8\alpha^+CD11c^+$ splenic cells were isolated from WT and TICAM-1 KO mice and infected with PV (MOI of 1). The expressions of type I IFNs and IFIT-1 were measured by RT-qPCR. Data are shown as means ± SD and are representative of three independent experiments.

in BM-Mf ~4 h after PV infection (Supplemental Fig. 3). Similarly, but less prominently, the profiles of type I IFN and IL-12p40 were observed in BM-DC (Fig. 6*A*, Supplemental Fig. 3) and $CD11c^+CD8^+$ splenic DC (Fig. 5*D*). Therefore, taken together, these results indicate that IL-12 and IFN-α/β are only minimally upregulated in splenic DC in a PV-dependent manner.

The production of IFN-α was determined by ELISA in the supernatant of PV-infected BM-Mf and BM-DC (Fig. 6*C*). BM-Mf prepared from WT mice generated higher amounts of IFN-α than did those from TICAM-$1^{-/-}$ mice. Although similar results were obtained with BM-DC, the effect of TICAM-1 depletion was not statistically significant (Fig. 6*C*).

NK cells and MEF do not play major roles in protection against PV infection

Using NK1.1-depleted mice, we tested the possible participation of NK cells in the protection of PVRtg mice from PV infection (Fig. 7). $NK1.1^+$ cells were depleted from mouse blood 1 d after injection (i.p.) of NK1.1 Ab into WT (Fig. 7*A*) and TICAM-$1^{-/-}$ mice. After PV challenge, WT mice inoculated with control saline and NK1.1 Ab survived similarly, whereas TICAM-$1^{-/-}$ mice were all killed by PV within 7.5 d irrespective of NK1.1 pretreatment (Fig. 7*B*). Hence, NK cell activation does not affect PV-derived death. The lack of TICAM-1 was also found to have no effect on the NK cell-mediated rescue of PV-infected mice.

Mouse fibroblasts are known to be a potential source of type I IFN (13). We therefore checked whether MEF induce type I IFN and protection against PV (Supplemental Fig. 4). MEF from WT PVRtg mice were susceptible to PV, with cell death being observed at an MOI of 1. MEF from TICAM-$1^{-/-}$ PVRtg mice were 1 log more susceptible to PV, with cell death occurring at an MOI of 0.1 (Supplemental Fig. 4*A*). IFN-β was upregulated in PV-infected MEF to only a slightly higher level in PVRtg MEF than in TICAM-$1^{-/-}$ PVRtg MEF (Supplemental Fig. 4*B*). These results suggested that the large difference in the PV survival rate between WT and TICAM-$1^{-/-}$ mice is not caused by NK cells or type I IFN induction by fibroblasts. The TICAM-1 pathway plays a key role for producing IFN-α/β in Mf/DC, but not in fibroblasts, during PV infection in PVRtg mice.

Discussion

In this study, we demonstrated that PV infection is exacerbated in TICAM-$1^{-/-}$ PVRtg mice. There are a number of RNA-sensing molecules that serve as anti-virus agents and function in a cell type-specific manner. Based on trials using gene-disrupted mice and human viruses, RIG-I has been reported to be essential for sensing infection by rhabdoviruses, influenza viruses, paramyxoviruses, and flaviviruses, whereas MDA5 is important for sensing picornavirus infection (13, 33). In previous studies on picornaviruses, however, only EMCV and several species of picornaviruses have been employed for the KO mice analyses (13). The essential role of type I IFN in PV tropism has been well characterized in PVRtg mice (34). To our knowledge, this study is the first to investigate the sensor that detects PV infection in PVRtg PV-sensitive mice. Because RIG-I and MDA5 use the adaptor IPS-1, we constructed an IPS-$1^{-/-}$ mouse strain for this

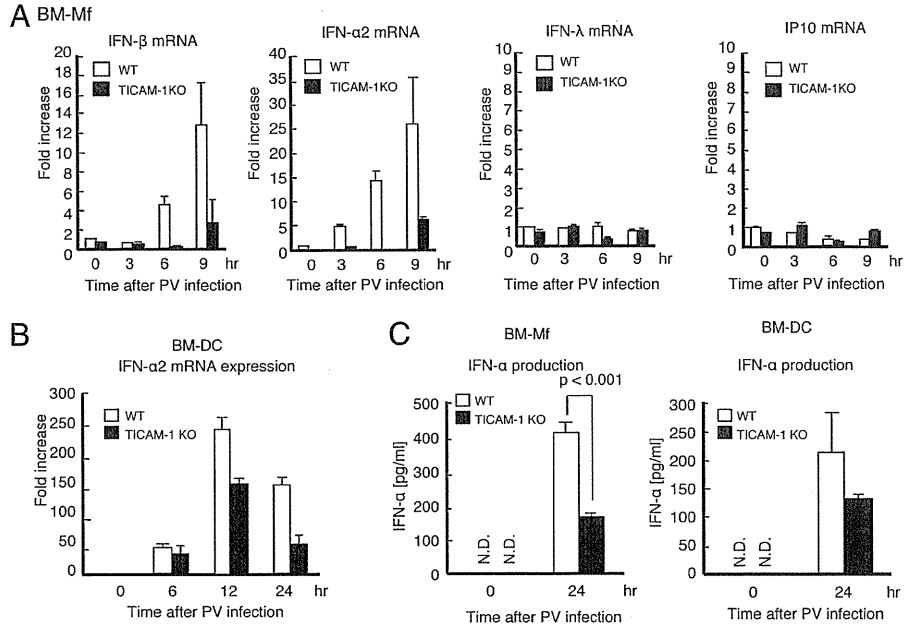

FIGURE 6. Production of type I IFN from BM-Mf and BM-DC. BM-Mf (*A*) and BM-DC (*B*) were prepared from BM cells with M-CSF and GM-CSF, respectively (32). The cells were infected with PV (MOI of 1), and the expression levels of IFN-β, IFN-α2, IFN-λ, and IP-10 were determined by RT-qPCR. *C*, IFN-α produced by PV-infected BM-Mf and BM-DC was measured by ELISA. BM-Mf and BM-DC were prepared from BM cells of WT and TICAM-1$^{-/-}$ mice as in *A* and *B*. Data are shown as means ± SD and are representative of three independent experiments.

study. Unexpectedly, however, IPS-1 was dispensable for protection against PV infection in vivo. This study, taken together with other reports (33, 35, 36), suggests that each virus species has its own strategy to evade host immune attack. This is true even in picornavirus subspecies. Although the IPS-1 pathway involving RIG-I and MDA5 is important for sensing and preventing cytoplasmic virus replication, other steps also participate in critical regulation of virus replication. PV infection is the case where MDA5 is not absolutely critical, but TICAM-1 is essential, for virus protection.

The TICAM-1 pathway participates in driving NK/CTL activation in DC/Mf (21, 37). This pathway is involved in type I IFN induction, as in the IPS-1 pathway, but cells expressing TLR3 are limited. The TLR3 distribution profile by flow cytometry confirms its expression in myeloid cells in mice (30). The TICAM-1 pathway converges with the IPS-1 pathway via the molecular complex of IRF-3–activating kinases (38), and therefore activation of the TICAM-1 pathway induces type I IFN and other IFN-inducible genes (39). Nevertheless, gene induction profiles differ between the TICAM-1 and IPS-1 pathways (40), which may explain the functional distinction between the sensor that is triggered in the virus-infected cells (MDA5/IPS-1) and the sensor that is required for DC/Mf to mount immune responses. Studying these gene functions will be an important issue for functional discrimination between the intrinsic versus extrinsic sensors.

RIG-1/MDA5 are distributed over almost all organs, including Mf/DC. An interesting point concerns what the function is of the IPS-1 pathway in Mf/DC. Without conditional KO mice, we have an experimental limit to discriminate between their intrinsic function that is triggered in PV-infected cells and the extrinsic function leading Mf/DC to driving the innate immune response. Because the TLR3/TICAM-1 pathway is conserved in Mf/DC, the CNS, fibroblasts, and epithelical cells, it is reasonable that their functions are rather specified in Mf/DC and the neuronal system in PV infection.

However, except several examples such as rhabdovirus (41) and hepatitis C virus (HCV) (32), no definitive evidence has been reported supporting the role of TLR3/TICAM-1 in anti-RNA virus function using KO mice, unlike IPS-1 (35, 36). In previous studies, we used RNA viruses and their mouse models of measles virus, respiratory syncitial virus, vesicular stomatitis virus, influenza virus, and rotavirus infection (12), but we were unable to demonstrate solid antiviral function of the TLR3/TICAM-1 pathway in these models (12). Accordingly, which type I IFN, IFN-inducible gene, NK cell, or CTL is an effector for antagonizing viral replication still remains uncharacterized. To our knowledge, the results of our present study first demonstrated that the TLR3/TICAM-1 pathway is indispensable for induction of the type I IFN effector, but not NK cell activation, which is a critical event in the elimination of virus-infected cells and host protection against PV. IL-12 and IFN-γ are not upregulated in splenic DC in a PV-dependent manner. Furthermore, CTL are unlikely to be involved in our present model, since they would not function within the time scale of several days after initial infection (42).

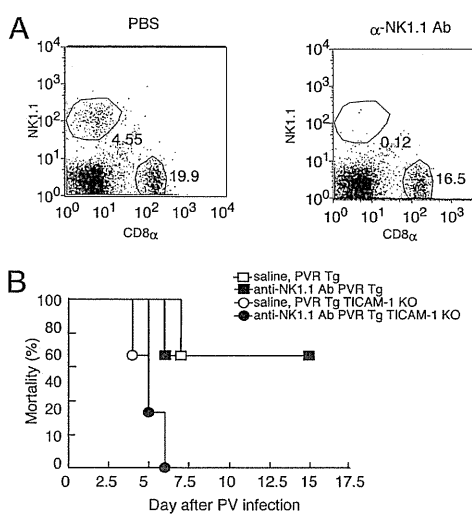

FIGURE 7. Effect of NK cells on mortality of PV-infected TICAM-1$^{-/-}$ PVRtg mice. *A*, To block the NK cell activity in mice, NK1.1 Ab or PBS (control) was i.p. injected into WT mice ($n \geq 6$). After 24 h, spleen cells were isolated from the mice and the fraction of NK1.1$^+$ cells was measured by FACS analysis. *B*, NK1.1 Ab or PBS was i.p. injected into WT and TICAM-1 KO mice. After 24 h, the mice were infected i.p. with PV, and survival was monitored for 15 d.

How PV circumvents host-inducible type I IFN is an intriguing point. Three lines of evidence have supported the presence of unique mechanisms by which PV infection abrogates MDA5-mediated type I IFN production by infected cells and accelerates TLR3-mediated DC maturation through phagocytosis of PV-infected cell debris. First, proteases encoded in the PV genome process the PV polyprotein to produce functional viral proteins (43). PV 2A and 3C proteases also contribute to the degradation of eIF4G (44) and TATA-binding protein (45), respectively, the cleavage of which induces the translational and transcriptional "shutoff" of host protein synthesis (28). Thus, blocking the synthesis of host cell proteins by PV involves stopping IFN production. Second, MDA5 is degraded in PV-infected cells in a proteasome- and caspase-dependent manner, resulting in the lack of type I IFN production (29). Third, PV-mediated apoptosis occurs in a caspase-dependent manner to disable infected cells from inducing an IFN response (46), with the MDA5-dependent innate response to PV infection becoming minimal within 3 h postinfection. Additionally, RIG-I is also cleaved by the viral protease 3C (47), and additional RIG-I functions are subsequently disrupted. Hence, the RIG-I/MDA5 functional time frames should be narrow and ineffective in PV-infected cells.

The hijacked cells release virions and die irrespective of blocking of the IPS-1 pathway. These infected cells are degrading into apoptotic debris containing virus dsRNA when RIG-I/MDA5 is ineffective at inducing IFN (48). Phagocytic internalization of this infected debris containing viral dsRNA into endosomes in Mf/DC is a critical event for TLR3 stimulation (37). If this is the case in PV-infected PVRtg mice, dsRNA-containing debris produced by apoptosis of PV-infected cells may play a major role in the activation of the TICAM-1 pathway in myeloid cells, as is the case for another positive-stranded RNA virus, HCV (32). In HCV studies, dead cells act as carriers of viral dsRNA to the endosomes of DC (32). HCV induces cellular immunity including NK activation driven by the DC TICAM-1 pathway. PV, however, barely induces NK cell activation.

The results of the present study were obtained using the PVRtg mouse model for human PV infection. Possible limitations of this model may include the fact that PV natural infection in humans occurs postinfection of the intestine by a low dose of PV and the PV mouse model is unable to reproduce this infectious route (27). The difference in PV infection between human and the PVRtg mouse might reflect the difference of the IFN-inducing system in humans and mice. However, the response to neurovirulence and death by PV infection occurs similarly in mice and humans. PVRtg mice are susceptible to neuronal infection and the IFNAR$^{-/-}$ phenotype further enhances systemic PV infection (27, 34). The G (Sabin vaccine) and A forms (WT) of PV, which harbor G or A residues in their stem-loop V structures, respectively, show different levels of toxicity or neurovirulence (49). The lower toxicity of the vaccine strain is due to suppression of PTB-mediated protein synthesis in the G form. These results are essentially reproducible in the PVRtg mouse model (50). Our findings further indicate the essential role of the TICAM-1 pathway in the PVRtg model system for the PV-mediated induction of type I IFN in vivo. How this finding is associated with PV-mediated paralytic death and aberrance in the neuronal system is an open question for further understanding the PV neurovirulence and host defense.

In studies on virus infection in neurons, there was no difference between TLR3$^{-/-}$ and WT mice in the brain of reovirus infection (51). TLR3$^{-/-}$ mice have less severe neuroinvasiveness and survive longer than do WT mice in rabies virus infection (41). Further extensive studies have been performed with West Nile virus (WNV). TLR3$^{-/-}$ or TICAM-1$^{-/-}$ mice became more resistant to WNV infection than did WT mice (52). Compared to these earlier results, a recent report showed that lack of TLR3 enhances WNV mortality and increases viral burden in the brain (53). TNF-α and IL-6 are induced for inflammation, and high IL-10 production causes an increase of mortality in WNV-infected mice (54). TICAM-1 signaling is undoubtedly involved in the modulation of these cytokine productions and WNV replication in the nervous system (53, 54). In patients with herpes simplex encephalitis, functional deficiency of TLR3 or TICAM-1 is a critical factor for disease progression (55). The TLR3 responses in the CNS may differ from those in the immune system we examined (54, 56). How PV infection modulates IFN/cytokine-inducing signaling in the nervous system is an interesting issue. The possibility remains that cytokines, such as TNF-α, IL-10, IL-12p40, and IFN-γ, might be associated with the removal of infectious cells as in other virus infections, and the antiviral function of TLR3 ligands in PV-infected mice requires further elucidation.

A picornavirus CBV activates the TLR3/TICAM-1–IFN-γ axis in host-infected cells to induce type II IFN (18). It is possible that CBV promotes TLR3-dependent IFN-γ induction in lymphocytes rather than the type I IFN-inducing pathway. In the model of PV infection, however, the TICAM-1 pathway does not contribute to type II IFN induction. These findings indicate that picornaviruses, that is, EMCV, CBV and PV, have independently evolved to adapt to the host innate immune system and cope with the IFN-inducing system. If this is the case, host responses against picornaviruses may not be unimodally raised by MDA5 but may provide differentially adapted strategies. EMCV tropism reported previously (13) is clearly distinct from those of other picornaviruses. In this article, we present evidence that PV infection is protected by the TICAM-1 pathway that extrinsically induces type I IFN. Virus-produced dsRNA may differentially act on host cells depending on each virus species and accomplish circumvention from host innate sensing systems, maintaining virus tropism.

Acknowledgments

We are grateful to Dr. A. Nomoto (University of Tokyo, Tokyo, Japan) and our laboratory members for invaluable discussions. We also thank Dr. D.M. Segal (National Institutes of Health, Bethesda, MD) for providing the anti-mouse TLR3 mAb and Drs. S. Akira (Osaka University, Osaka, Japan) and T. Taniguchi (University of Tokyo) for providing TLR3$^{-/-}$ and IRF3/7$^{-/-}$ mice, respectively, for this study.

Disclosures

The authors have no financial conflicts of interest.

References

1. Takeuchi, O., and S. Akira. 2009. Innate immunity to virus infection. *Immunol. Rev.* 227: 75–86.
2. Malathi, K., B. Dong, M. Gale, Jr., and R. H. Silverman. 2007. Small self-RNA generated by RNase L amplifies antiviral innate immunity. *Nature* 448: 816–819.
3. Oshiumi, H., M. Matsumoto, K. Funami, T. Akazawa, and T. Seya. 2003. TICAM-1, an adaptor molecule that participates in Toll-like receptor 3-mediated interferon-β induction. *Nat. Immunol.* 4: 161–167.
4. Yamamoto, M., S. Sato, H. Hemmi, K. Hoshino, T. Kaisho, H. Sanjo, O. Takeuchi, M. Sugiyama, M. Okabe, K. Takeda, and S. Akira. 2003. Role of adaptor TRIF in the MyD88-independent Toll-like receptor signaling pathway. *Science* 301: 640–643.
5. Hoebe, K., X. Du, P. Georgel, E. Janssen, K. Tabeta, S. O. Kim, J. Goode, P. Lin, N. Mann, S. Mudd, et al. 2003. Identification of Lps2 as a key transducer of MyD88-independent TIR signalling. *Nature* 424: 743–748.
6. Akira, S. 2003. Toll-like receptor signaling. *J. Biol. Chem.* 278: 38105–38108.
7. Matsumoto, M., and T. Seya. 2008. TLR3: interferon induction by double-stranded RNA including poly(I:C). *Adv. Drug Deliv. Rev.* 60: 805–812.
8. Funami, K., M. Sasai, Y. Ohba, H. Oshiumi, T. Seya, and M. Matsumoto. 2007. Spatiotemporal mobilization of Toll/IL-1 receptor domain-containing adaptor molecule-1 in response to dsRNA. *J. Immunol.* 179: 6867–6872.
9. Funami, K., M. Sasai, H. Oshiumi, T. Seya, and M. Matsumoto. 2008. Homo-oligomerization is essential for Toll/interleukin-1 receptor domain-containing

adaptor molecule-1-mediated NF-κB and interferon regulatory factor-3 activation. *J. Biol. Chem.* 283: 18283–18291.
10. Yoneyama, M., M. Kikuchi, T. Natsukawa, N. Shinobu, T. Imaizumi, M. Miyagishi, K. Taira, S. Akira, and T. Fujita. 2004. The RNA helicase RIG-I has an essential function in double-stranded RNA-induced innate antiviral responses. *Nat. Immunol.* 5: 730–737.
11. Yoneyama, M., M. Kikuchi, K. Matsumoto, T. Imaizumi, M. Miyagishi, K. Taira, E. Foy, Y. M. Loo, M. Gale, Jr., S. Akira, et al. 2005. Shared and unique functions of the DExD/H-box helicases RIG-I, MDA5, and LGP2 in antiviral innate immunity. *J. Immunol.* 175: 2851–2858.
12. Matsumoto, M., H. Oshiumi, and T. Seya. 2011. Antiviral responses induced by the TLR3 pathway. *Rev. Med. Virol.* 21: 67–77.
13. Kato, H., O. Takeuchi, S. Sato, M. Yoneyama, M. Yamamoto, K. Matsui, S. Uematsu, A. Jung, T. Kawai, K. J. Ishii, et al. 2006. Differential roles of MDA5 and RIG-I helicases in the recognition of RNA viruses. *Nature* 441: 101–105.
14. Tabeta, K., P. Georgel, E. Janssen, X. Du, K. Hoebe, K. Crozat, S. Mudd, L. Shamel, S. Sovath, J. Goode, et al. 2004. Toll-like receptors 9 and 3 as essential components of innate immune defense against mouse cytomegalovirus infection. *Proc. Natl. Acad. Sci. USA* 101: 3516–3521.
15. Baltimore, D., Y. Becker, and J. E. Darnell. 1964. Virus-specific double-stranded RNA in poliovirus-infected cells. *Science* 143: 1034–1036.
16. Nomoto, A., B. Detjen, R. Pozzatti, and E. Wimmer. 1977. The location of the polio genome protein in viral RNAs and its implication for RNA synthesis. *Nature* 268: 208–213.
17. Gitlin, L., W. Barchet, S. Gilfillan, M. Cella, B. Beutler, R. A. Flavell, M. S. Diamond, and M. Colonna. 2006. Essential role of mda-5 in type I IFN responses to polyriboinosinic:polyribocytidylic acid and encephalomyocarditis picornavirus. *Proc. Natl. Acad. Sci. USA* 103: 8459–8464.
18. Negishi, H., T. Osawa, K. Ogami, X. Ouyang, S. Sakaguchi, R. Koshiba, H. Yanai, Y. Seko, H. Shitara, K. Bishop, et al. 2008. A critical link between Toll-like receptor 3 and type II interferon signaling pathways in antiviral innate immunity. *Proc. Natl. Acad. Sci. USA* 105: 20446–20451.
19. Ren, R. B., F. Costantini, E. J. Gorgacz, J. J. Lee, and V. R. Racaniello. 1990. Transgenic mice expressing a human poliovirus receptor: a new model for poliomyelitis. *Cell* 63: 353–362.
20. Koike, S., C. Taya, T. Kurata, S. Abe, I. Ise, H. Yonekawa, and A. Nomoto. 1991. Transgenic mice susceptible to poliovirus. *Proc. Natl. Acad. Sci. USA* 88: 951–955.
21. Akazawa, T., T. Ebihara, M. Okuno, Y. Okuda, M. Shingai, K. Tsujimura, T. Takahashi, M. Ikawa, M. Okabe, N. Inoue, et al. 2007. Antitumor NK activation induced by the Toll-like receptor 3-TICAM-1 (TRIF) pathway in myeloid dendritic cells. *Proc. Natl. Acad. Sci. USA* 104: 252–257.
22. Honda, K., H. Yanai, H. Negishi, M. Asagiri, M. Sato, T. Mizutani, N. Shimada, Y. Ohba, A. Takaoka, N. Yoshida, and T. Taniguchi. 2005. IRF-7 is the master regulator of type-I interferon-dependent immune responses. *Nature* 434: 772–777.
23. Kato, H., O. Takeuchi, E. Mikamo-Satoh, R. Hirai, T. Kawai, K. Matsushita, A. Hiiragi, T. S. Dermody, T. Fujita, and S. Akira. 2008. Length-dependent recognition of double-stranded ribonucleic acids by retinoic acid-inducible gene-I and melanoma differentiation-associated gene 5. *J. Exp. Med.* 205: 1601–1610.
24. Hornung, V., J. Ellegast, S. Kim, K. Brzózka, A. Jung, H. Kato, H. Poeck, S. Akira, K. K. Conzelmann, M. Schlee, et al. 2006. 5′-Triphosphate RNA is the ligand for RIG-I. *Science* 314: 994–997.
25. Pichlmair, A., O. Schulz, C. P. Tan, T. I. Näslund, P. Liljeström, F. Weber, and C. Reis e Sousa. 2006. RIG-I-mediated antiviral responses to single-stranded RNA bearing 5′-phosphates. *Science* 314: 997–1001.
26. Nakajima, A., K. Nishimura, Y. Nakaima, T. Oh, S. Noguchi, T. Taniguchi, and T. Tamura. 2009. Cell type-dependent proapoptotic role of Bcl2L12 revealed by a mutation concomitant with the disruption of the juxtaposed *Irf3* gene. *Proc. Natl. Acad. Sci. USA* 106: 12448–12452.
27. Ohka, S., H. Igarashi, N. Nagata, M. Sakai, S. Koike, T. Nochi, H. Kiyono, and A. Nomoto. 2007. Establishment of a poliovirus oral infection system in human poliovirus receptor-expressing transgenic mice that are deficient in α/β interferon receptor. *J. Virol.* 81: 7902–7912.
28. Racaniello, V. R. 2007. Picornaviridae: the viruses and their replication. In *Fields Virology*, 5th Ed. D. M. Knipe and P. M. Howley, eds. Lippincott Williams & Wilkins, Philadelphia, p. 795–838.
29. Barral, P. M., J. M. Morrison, J. Drahos, P. Gupta, D. Sarkar, P. B. Fisher, and V. R. Racaniello. 2007. MDA-5 is cleaved in poliovirus-infected cells. *J. Virol.* 81: 3677–3684.
30. Jelinek, I., J. N. Leonard, G. E. Price, K. N. Brown, A. Meyer-Manlapat, P. K. Goldsmith, Y. Wang, D. Venzon, S. L. Epstein, and D. M. Segal. 2011. TLR3-specific double-stranded RNA oligonucleotide adjuvants induce dendritic cell cross-presentation, CTL responses, and antiviral protection. *J. Immunol.* 186: 2422–2429.
31. Matsumoto, M., K. Funami, M. Tanabe, H. Oshiumi, M. Shingai, Y. Seto, A. Yamamoto, and T. Seya. 2003. Subcellular localization of Toll-like receptor 3 in human dendritic cells. *J. Immunol.* 171: 3154–3162.
32. Ebihara, T., M. Shingai, M. Matsumoto, T. Wakita, and T. Seya. 2008. Hepatitis C virus-infected hepatocytes extrinsically modulate dendritic cell maturation to activate T cells and natural killer cells. *Hepatology* 48: 48–58.
33. Loo, Y. M., J. Fornek, N. Crochet, G. Bajwa, O. Perwitasari, L. Martinez-Sobrido, S. Akira, M. A. Gill, A. García-Sastre, M. G. Katze, and M. Gale, Jr. 2008. Distinct RIG-I and MDA5 signaling by RNA viruses in innate immunity. *J. Virol.* 82: 335–345.
34. Ida-Hosonuma, M., T. Iwasaki, T. Yoshikawa, N. Nagata, Y. Sato, T. Sata, M. Yoneyama, T. Fujita, C. Taya, H. Yonekawa, and S. Koike. 2005. The α/β interferon response controls tissue tropism and pathogenicity of poliovirus. *J. Virol.* 79: 4460–4469.
35. Kumar, H., T. Kawai, H. Kato, S. Sato, K. Takahashi, C. Coban, M. Yamamoto, S. Uematsu, K. J. Ishii, O. Takeuchi, and S. Akira. 2006. Essential role of IPS-1 in innate immune responses against RNA viruses. *J. Exp. Med.* 203: 1795–1803.
36. Sun, Q., L. Sun, H. H. Liu, X. Chen, R. B. Seth, J. Forman, and Z. J. Chen. 2006. The specific and essential role of MAVS in antiviral innate immune responses. *Immunity* 24: 633–642.
37. Schulz, O., S. S. Diebold, M. Chen, T. I. Näslund, M. A. Nolte, L. Alexopoulou, Y. T. Azuma, R. A. Flavell, P. Liljeström, and C. Reis e Sousa. 2005. Toll-like receptor 3 promotes cross-priming to virus-infected cells. *Nature* 433: 887–892.
38. Sasai, M., M. Shingai, K. Funami, M. Yoneyama, T. Fujita, M. Matsumoto, and T. Seya. 2006. NAK-associated protein 1 participates in both the TLR3 and the cytoplasmic pathways in type I IFN induction. *J. Immunol.* 177: 8676–8683.
39. Oshiumi, H., M. Sasai, K. Shida, T. Fujita, M. Matsumoto, and T. Seya. 2003. TIR-containing adapter molecule (TICAM)-2, a bridging adapter recruiting to Toll-like receptor 4 TICAM-1 that induces interferon-beta. *J. Biol. Chem.* 278: 49751–49762.
40. Ueta, M., T. Kawai, N. Yokoi, S. Akira, and S. Kinoshita. 2011. Contribution of IPS-1 to polyI:C-induced cytokine production in conjunctival epithelial cells. *Biochem. Biophys. Res. Commun.* 404: 419–423.
41. Ménager, P., P. Roux, F. Mégret, J. P. Bourgeois, A. M. Le Sourd, A. Danckaert, M. Lafage, C. Préhaud, and M. Lafon. 2009. Toll-like receptor 3 (TLR3) plays a major role in the formation of rabies virus Negri bodies. *PLoS Pathog.* 5: e1000315.
42. Sigal, L. J., S. Crotty, R. Andino, and K. L. Rock. 1999. Cytotoxic T-cell immunity to virus-infected non-haematopoietic cells requires presentation of exogenous antigen. *Nature* 398: 77–80.
43. Nicklin, M. J., H. G. Kräusslich, H. Toyoda, J. J. Dunn, and E. Wimmer. 1987. Poliovirus polypeptide precursors: expression in vitro and processing by exogenous 3C and 2A proteinases. *Proc. Natl. Acad. Sci. USA* 84: 4002–4006.
44. Kräusslich, H. G., M. J. Nicklin, H. Toyoda, D. Etchison, and E. Wimmer. 1987. Poliovirus proteinase 2A induces cleavage of eucaryotic initiation factor 4F polypeptide p220. *J. Virol.* 61: 2711–2718.
45. Clark, M. E., P. M. Lieberman, A. J. Berk, and A. Dasgupta. 1993. Direct cleavage of human TATA-binding protein by poliovirus protease 3C in vivo and in vitro. *Mol. Cell. Biol.* 13: 1232–1237.
46. Belov, G. A., L. I. Romanova, E. A. Tolskaya, M. S. Kolesnikova, Y. A. Lazebnik, and V. I. Agol. 2003. The major apoptotic pathway activated and suppressed by poliovirus. *J. Virol.* 77: 45–56.
47. Barral, P. M., D. Sarkar, P. B. Fisher, and V. R. Racaniello. 2009. RIG-I is cleaved during picornavirus infection. *Virology* 391: 171–176.
48. Barco, A., E. Feduchi, and L. Carrasco. 2000. Poliovirus protease $3C^{pro}$ kills cells by apoptosis. *Virology* 266: 352–360.
49. Kawamura, N., M. Kohara, S. Abe, T. Komatsu, K. Tago, M. Arita, and A. Nomoto. 1989. Determinants in the 5′ noncoding region of poliovirus Sabin 1 RNA that influence the attenuation phenotype. *J. Virol.* 63: 1302–1309.
50. Koike, S., H. Horie, Y. Sato, I. Ise, C. Taya, T. Nomura, I. Yoshioka, H. Yonekawa, and A. Nomoto. 1993. Poliovirus-sensitive transgenic mice as a new animal model. *Dev. Biol. Stand.* 78: 101–107.
51. Edelmann, K. H., S. Richardson-Burns, L. Alexopoulou, K. L. Tyler, R. A. Flavell, and M. B. A. Oldstone. 2004. Does Toll-like receptor 3 play a biological role in virus infections? *Virology* 322: 231–238.
52. Wang, T., T. Town, L. Alexopoulou, J. F. Anderson, E. Fikrig, and R. A. Flavell. 2004. Toll-like receptor 3 mediates West Nile virus entry into the brain causing lethal encephalitis. *Nat. Med.* 10: 1366–1373.
53. Daffis, S., M. A. Samuel, M. S. Suthar, M. Gale, Jr., and M. S. Diamond. 2008. Toll-like receptor 3 has a protective role against West Nile virus infection. *J. Virol.* 82: 10349–10358.
54. Bai, F., T. Town, F. Qian, P. Wang, M. Kamanaka, T. M. Connolly, D. Gate, R. R. Montgomery, R. A. Flavell, and E. Fikrig. 2009. IL-10 signaling blockade controls murine West Nile virus infection. *PLoS Pathog.* 5: e1000610.
55. Zhang, S. Y., E. Jouanguy, S. Ugolini, A. Smahi, G. Elain, P. Romero, D. Segal, V. Sancho-Shimizu, L. Lorenzo, A. Puel, et al. 2007. TLR3 deficiency in patients with herpes simplex encephalitis. *Science* 317: 1522–1527.
56. Préhaud, C., F. Mégret, M. Lafage, and M. Lafon. 2005. Virus infection switches TLR-3-positive human neurons to become strong producers of beta interferon. *J. Virol.* 79: 12893–12904.